Analysis of Eclipsing Binary Exoplanets and Analysis of Transit Timing Variation from TESS data

Lo Tinfei and Fu Jiani

August 8, 2022

Key Words: TESS data, Transit timing variation, Eclipsing binary star, Exoplanets

Abstract

This study uses openly available TESS (Transiting Exoplanet Sky Survey) data with the aim to detect evidence for potential exoplanet transits in a eclipsing binary system. Using Python package lightkurve, we discuss the characteristics of an eclipsing binary star's light curve in determining the classification of a system. In addition, we also study phenomena on a light curve that indicates the existence of a potential exoplanet. Although this investigation yields a null result, finding no conclusive evidence suggesting the present of exoplanet transits in known eclipsing binaries using TESS data, we explored in depth the physical properties of binary star system TIC 7720507, identifying strong methods for explanatory stellar research.

1 Introduction

The field of exoplanets detection has been transformed in the past two decades from being dominated by philosophical and theoretical considerations to having full utilisation of advanced and precise astrophysicals. Launched on a SpaceX Falcon 9 Rocket on 18th of April, 2018, the Transiting Exoplanet Survey Satellite (TESS) observed over 200,000 stars stars during its two-year prime mission with the aim to discover exoplanets transiting nearby, bright stars with a focus of Earth and Super-Earth sized planets. Similarly, NASA's Kepler during its 4-years operational period, observed 530,506 stars and detected 2,662 planets, detecting 2,878 eclipsing binary stars. (Kuiper, 1938) Modern methods of exoplanet detection varies, but known exoplanets are discovered via observing the transit method (Pepe et al.), which can be observed when a planet passes through between a star and the observer on Earth, thus creating a change in apparent luminosity and a dip in its light curve. A transit event can enlighten researchers on the planet's fundamental properties such as mass, radius and orbit, its planetary dynamics including interplanetary interactions, moons and tides, but also information about it's atmospheric composition and emission spectrum; these information is not always available to the researchers with the TESS data alone, therefore objects of interest usually demand further follow-up studies.

This study focuses on eclipsing binaries and circumbinary exoplanets. Binary stars are abundant in the universe, with most estimates suggesting that the majority of stars in the universe are in binary or more complex systems; these systems contain~~s~~ two or more stars gravitationally bound~~ed~~ together that orbit a common centre of mass. They are vital to astrophysical research because the laws of motions are clearly defined for binary stars, they are used to calibrate the Hertzsprung-Russell diagram of stellar evolution and are ideal as distance estimators as the absolute luminosity can be easy deduced. Changes in the observed flux of eclipsing binaries as a function of time provide further information regarding the physical parameters of the stellar system. (Barbuzano)

Therefore the seeming~~ly~~ absence of known exoplanets in binary star systems may feel counter-intuitive knowing the relative copiousness of such systems in the Milky Way galaxy. In fact, only around 400 exoplanets around binary star systems has been confirmed — a small portion compared to the over 5000 exoplanets confirmed in total considering such systems' relative abundance in the universe. Some astronomers credit this unexpected phenomena to the inherent instability of exoplanets in binary systems, while others planets in multiple systems could be as common as around single stars but current astronomical detection are not accounting them due to substantial observational biases. Not only does analysis of exoplanets in binary systems introduce technical

challenges, but when using the transit method, the changes in observed luminosity of an exoplanet tend to be small-scaled compared with those of stars on light curves. For this reason, under constraints with time and computational capacity, visual detection of exoplanet transits still proves meretricious.

This studies uses openly available TESS data for eclipsing binary stars and circumbinary exoplanets to plot and analysis its light curves with Python package lightkurve. Building on a existing and extensive catalogue of observed eclipsing binary stars from TESS data which noted 4584 eclipsing binaries during the first 26 sectors from Prsa et al., which was later appended by 360 new candidates by Howard et al. in 2022, we aimed to gain a better understanding of the mechanisms of eclipsing binary stars and comparing our obtained information regarding the star's physical properties to available data to gain insight on the accuracy of data based purely on TESS light curve analysis on transits. Furthermore, we hope to visually identify the presence of possible exoplanet transits among the binary light curves.

2 Method

2.1 TESS Data Selection

Since the focus of this investigation is to identify an exoplanet transit in binary star system from the TESS data on eclipsing binary stars, we referenced a catalogue of over 4000 identified eclipsing binaries by Prsa et al. (in conjunction with 370 additional binaries discovered by Howard et al.) from the TESS Mission available data. By using previous studies that already identified potential candidates, we can increase the possibility of detecting an exoplanet in a binary system by narrowing our focus.

2.2 Lightkurve Programming

To study the behavior of a star, we use the TESS data selected by Prsa et al. and the programming package of lightkurve by **?**to analyzing astronomical flux time series data to find transits.

The investigation first uses an object ID number assigned by TESS, which produce a list of celestial bodies as shown by, and select an object to study.

```
In [2]: result = lk.search_lightcurve('TIC 7720507', mission = 'Tess')
        result
```

Out[2]: SearchResult containing 7 data products.

#	mission	year	author	exptime	target_name	distance
				s		arcsec
0	TESS Sector 25	2020	SPOC	120	7720507	0.0
1	TESS Sector 25	2020	TESS-SPOC	1800	7720507	0.0
2	TESS Sector 25	2020	QLP	1800	7720507	0.0
3	TESS Sector 26	2020	SPOC	120	7720507	0.0
4	TESS Sector 26	2020	TESS-SPOC	1800	7720507	0.0
5	TESS Sector 26	2020	QLP	1800	7720507	0.0
6	TESS Sector 40	2021	SPOC	120	7720507	0.0

Figure 1: A list of celestial bodies produced by the lightkurve package for TIC 7720507

After selecting a system, we first produce a graph showing a star's instantaneous flux to time to observe dips indicating transits, shown by figure 4 within a relatively large time period. When discovering potential or a pattern of periodic dips, we can magnify the lightcurve by selecting a specific time period in which dips potentially occur, shown by figure 3, reducing the possibility of

missing exoplanets by avoiding human limitation. If an apparent dip is observed, the investigation uses the Box Least Squares (BLS) Periodogram method, a statistical tool that demonstrates various quantities, to produce a graph of BLS power versus time. Then, uses the BLS tool to determine a star's transiting period and duration.

For the visual identification of transiting exoplanets we choose to mainly rely on the raw lightcurve before phase-folding as we expect the changes in luminosity of the transiting exoplanet to demonstrate a different period to the preexisting pattern of the eclipsing binary stars on the lightcurve. For this reason, phase-folding and further programs performed on the lightcurves are minimised for exoplanet detection in this investigation. The unpredictability of astronomical observations provided to pose a great challenge towards exoplanet detection in binary systems as unexpected behaviour in the lightcurves may instead be credits to systemic error with TESS, 'postage stars' where the changes in luminosity is a result of the star's motion in and out of the picture frame, active solar flares, or changes in luminosity with inherent variable stars.

For exoplanet detection in binary systems, in order to be efficient with both limited time and computational resources, we paired visual identification of binary systems using processed light curves available on Prša et al. 2021 followed by further analysis of suspicious systems with primary analysis of light curves using Python with TESS data. We also fully utilised available astronomical databases such as SIMBAD when considering suspicious systems as it is difficult if not impossible extract sufficient information regarding a multiple star system with its eclipsing light curve, including the stars' classification to rule out the possibility of other disturbances in the flux such as vigorous stellar activity. This approach has proven effective in the case of TIC xxxxx, where as shown in figure **??**, later research proves that the case is an outlier.

2.3 Relevant Equations

Period and transit duration are directly calculated by the BLS method in lightkurve by folding the lightkurve shown by Figure 3. Using the two values, we can determine basic properties of a~~n~~ star using relevant equations as shown the section of equations.

From a star's light curve, we can also determine its relative size. The fractional depth of a transit indicates relative size of a star with respect to its orbiting object in terms of radius(Teske et al. (2020)), expressed by the equation 2.3.1, where R_* is the radius of the star, and R_p is the radius of the orbiting object.

$$\delta = \left(\frac{R_*}{R_p}\right)^2. \tag{2.3.1}$$

Apparent magnitude is a measure of the brightness of a star or other astronomical object observed from Earth, and absolute magnitude is a measure of the intrinsic luminosity of a celestial body viewed from 10 parsec away. The relation between the two quantities are shown by 2.3.2 Its relation to the absolute magnitude is shown by equation 2.3.2, where m is the star's apparent magnitude, and M is its absolute magnitude, and d is distance in parsecs.

$$M = m - 5\left(\log_{10}\frac{d}{10\,\mathrm{pc}}\right), \tag{2.3.2}$$

Parallax is the displacement or difference in the apparent position of an object when viewed from two lines of sight, producing an angle between two lines' intersection and allowing an astronomer to determine the object's distance using trigonometry. The relation between a star's distance and parallax angle is illustrated by equation 2.3.3, a quantity commonly detected by the Gaia mission, where d is the distance in parsecs, and p refers to the star's parallax angle.

$$d = \frac{1}{p}, \tag{2.3.3}$$

After knowing a celestial object's absolute luminosity and temperature, we can approximate the radius using the Hertzsprung–Russell diagram, indicated by a diagonal line running that represents locations where stars have the have the same radius.

Stefan Boltzmann law proposes that the radian power by a black-body directly proportional to the fourth power of the object's temperature in Kelvin (Fisenko and Ivashov (2009)). Using

the Stefan-Boltzmann, we can express an object's luminosity by temperature and radius, we can determine a star's radius as shown by equation 2.3.4.

$$L_* = 4\pi {R_*}^2 \sigma T^4, \tag{2.3.4}$$

L_s stands for the luminosity emitted from the surface of an astronomical object, R_s stands for the radius of the star, and σ refers to the value of Stefan-Boltzmann constant, which has a value of $5.67 \times 10^{-8}\,\mathrm{Wm^{-2}K^{-4}}$.

Kepler's third law states that the square of a star's period is directly proportional to the cubic semi-major axis of its orbit, shown by 2.3.5. P is the period in seconds, G is the gravitational constant with a value of $6.67 \times 10^{-11}\,\mathrm{m^3kg^{-1}s^{-2}}$, and a is the semi-major axis in meters.

$$P^2 = \frac{4\pi^2}{(GM)} a^3, \tag{2.3.5}$$

Without knowing the semi-major axis and the mass of the star, we can determine the density of a celestial object object using approximations, adapted from Richmond.

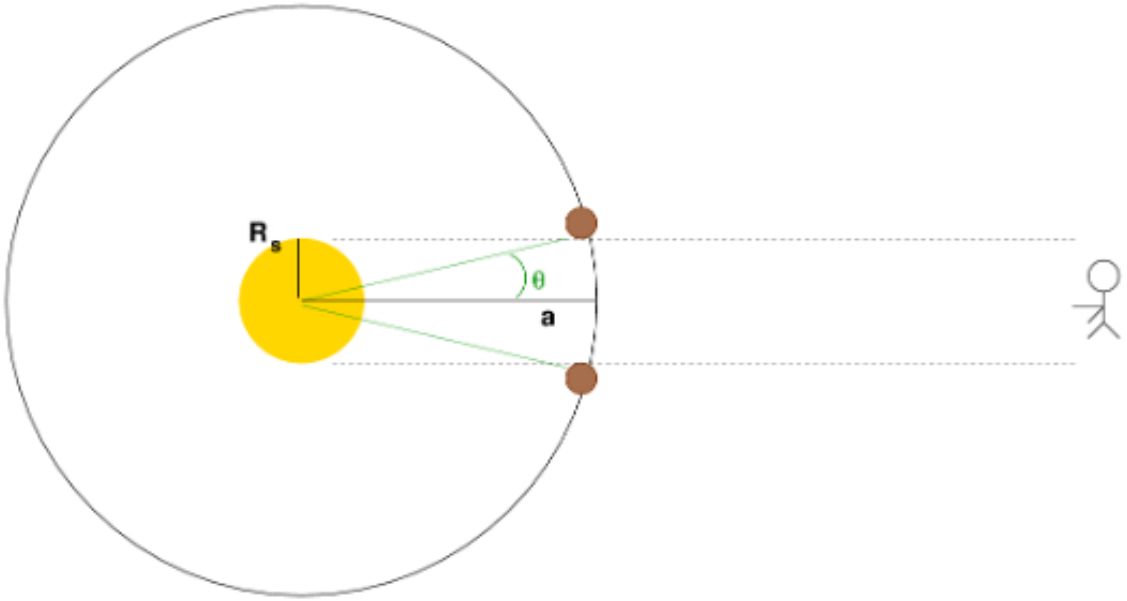

Figure 2: Approximation of a celestial object's density using Kepler's third law, adopted from Richmond

.

Illustrated by figure 2, $\tan\theta$ is equal to the ratio of radius of the star, R_s to the value of the orbit's semi-major axis. Since θ is a small value, we can approximate that $\tan\theta$ is equal to θ, shown by equation 2.3.6.

$$\theta \approx \frac{R_*}{a}. \tag{2.3.6}$$

$$\frac{\theta}{\pi} = \frac{T}{P} = \frac{R_*}{\pi a}, \tag{2.3.7}$$

where R stands for the radius of the star, and a stands for the semi-major axis.

Since mass is equal to density multiplied by volume, the equation for Kepler's law can be further simplified.

$$P^2 = \frac{4\pi^2}{\frac{4}{3}\pi G\rho_s}\left(\frac{a^3}{R_*^3}\right) = \frac{4\pi^2}{\frac{4}{3}\pi G\rho_s}\left(\frac{P^3}{\pi^3 T^3}\right). \tag{2.3.8}$$

Simplifying equation, density is equal to:

$$\rho_s = \frac{3P}{G\pi^2 T^3}. \tag{2.3.9}$$

3 Analysis

3.1 Light Curve Analysis

By selecting a particular binary system without a transiting exoplanet, we hope to gain better insight of eclipsing binary stars, its corresponding light curves, and information regarding the system that can be extrapolated from the TESS data.

TIC 7720507 is an eclipsing binary star, observed by the TESS mission in 2015 in sector 25; it is a particularly useful example as it demonstrates a defining example of the transits of an eclipsing binary star and is not victim to systematic errors. Using TESS data to produce a light curve graph of the star's flux to time, the graph can be zoomed, as shown by 5,to further study its behavior. From 4, we can clearly that the star (TIC 7720507)'s flux changes periodically with two dips with different depths. To better observe the dip pattern and confirm if the system is eclipsing binary, we select the time interval of 2012 to 2014 to zoom in the image, shown by 4.

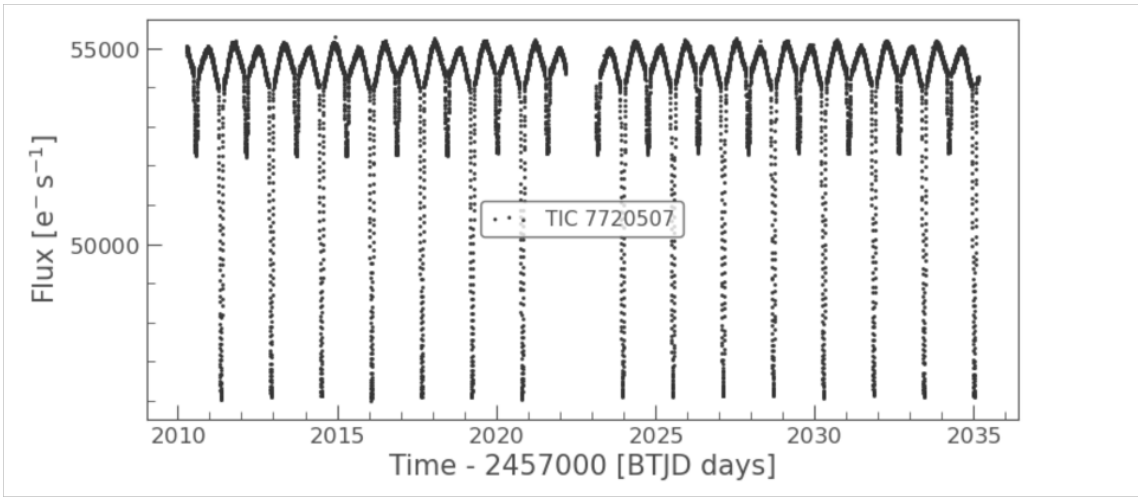

Figure 3: Light curve of TIC 7720507, showing the graph of flux versus time in BTJD days

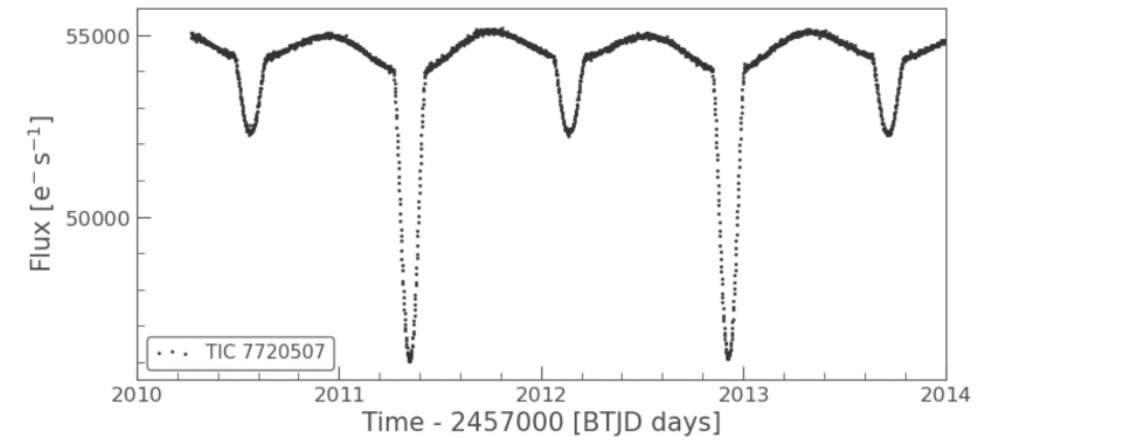

Figure 4: Zoomed-in light curve of TIC 7720507 during, showing both primary and secondary eclipses: the selected time interval is 2010 to 2015 BTJD days

As shown by figure 4, the light curve of TIC 2457000 produces transits with two different depths, clearly indicating that the system is an eclipsing binary as a dimmer and brighter star block orbit around each other. Dips with a greater depth represent primary eclipses, meaning that the secondary star blocks the primary star, so the eclipse is deep since more lights are blocked. On the other hand, dips with a small flux change indicate secondary eclipses, meaning that the brighter star blocks the dimmer star, so the eclipse is less deep since fewer lights are blocked (Tran et al. (2013)). When flux reaches its minimum value, dips in the figure become points during transit duration. Therefore, we can conclude that two eclipsing stars have a similar size, so the

duration of primary and secondary eclipses lasts for a limited period, causing the minimum flux to be a point.

Between primary and secondary eclipses, the graph of flux versus time curves increases its brightness after eclipses and then decreases its value. While orbital revolutions cause transit, fluctuations in brightness are due to rotations of one object in the system. Since TIC 7720507 is an eclipsing binary star system, the change is primarily caused by its companion stars, causing primary and secondary stars to be tidally locked. This can be seen in the curved nature of the light curve, reflecting the changes in flux as the stars are not perfectly symmetrical shapes due to tidal forces(Giuricin et al. (1984)).

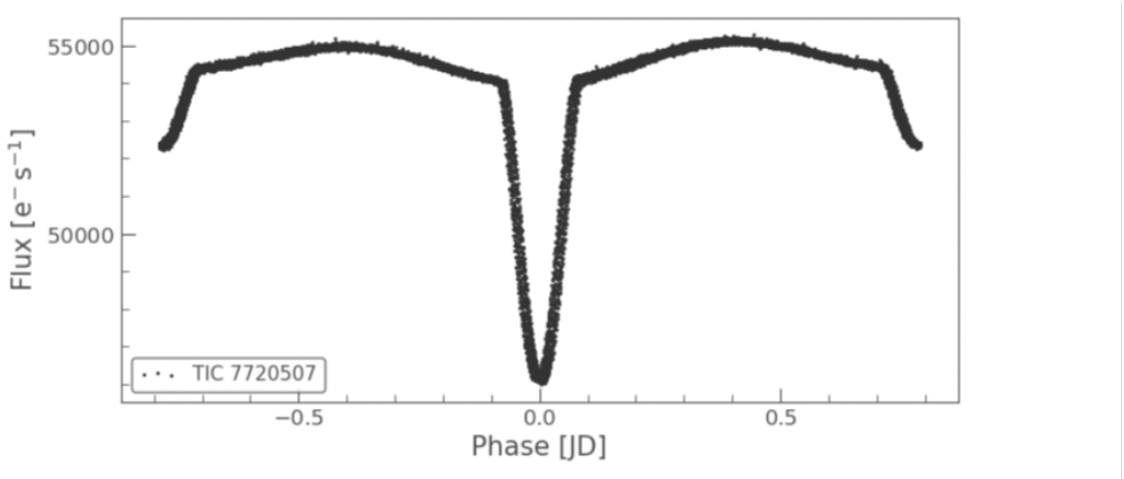

Figure 5: One complete transit phase of TIC 7720507 after phase folding

3.2 Primary Star Analysis

The fractional depth, δ, of a transit is equal to the relative size of a star. However, since TIC 7720507 is an eclipsing binary star, the transit depth is equal to the ratio square of the radius of TIC 7720507 to its companion star.

As a primary eclipse occurs, the fractional depth is equal to the squared ratio of the brighter star's radius to its companion star, which is the dimmer one. As a secondary eclipse occurs, the fractional depth is equal to the squared ratio of the fainter star's radius to the lighter star. From figure 7, we can see that the secondary eclipse has a fractional depth of 0.91, expressed by equation 3.2.1 revealing that two binary stars' have a similar radius, explaining that point transit in figure 3.

$$\delta = \left(\frac{R_{\text{fainter}}}{R_{\text{brighter}}}\right)^2 = 0.91 \tag{3.2.1}$$

Using the BLS (Box Least Squares), we can calculate the period and transit duration of TIC 7720507, which produce a value of 1.5785785785785786 and 0.1 days. Converting the two quantities into second, period P is equal to 136389.19 seconds, and duration T is equal to 8640 seconds. Knowing the period of the sun is 24.47 days, we can convert the star's period in the solar scale used by astronomers.

$$P_s = 1.58\text{days} = 136389.19\text{sec} = 0.065\text{P}_\odot \tag{3.2.2}$$

Obtaining results from the lighkuve program, we also use the astronomical database of SIMBAD to find the ID number of TIC 7720507 by the Gaia mission, 2121683951252006016, to find its parallax angle. Based on available information from the astronomical database and the Gaia mission, TIC 7720507 has a parallax of 5.7123 milliarcsecond and an apparent magnitude of 8.65438, allowing us to determine its distance by equation 2.3.3 and absolute magnitude.

$$d = \frac{1}{0.0057123} = 175.06\text{pc} \tag{3.2.3}$$

Then, we can calculate the star's absolute magnitude using equation 2.3.2, which gives us a result of 2.438

$$M = 8.65438 - 5\left(\log_{10}\frac{175.06}{10}\right) = 2.438 = 0.505M_{\odot} \tag{3.2.4}$$

Using equation 2.3.9, density of the star is equal to:

$$\rho_s = 963.68\text{kgm}^{-3} = 0.69\rho_{\odot} \tag{3.2.5}$$

To further determine basic properties of the star, TIC 7720507, we use the Hertzsprung-Russell diagram, we can determine the star's classification based on known information by . From the the Hertzsprung-Russell diagram, we can see that TIC 7720507 is a main sequence star with a yellow white color and a radius of 0.80 solar radii.

$$R_s = 0.80R\odot \tag{3.2.6}$$

Ignoring possible irregularities in the star's shape and approximate the object into a perfect sphere, we can calculate its volume using the obtained values of radius and density from 2.3.9 and 3.2.6.

$$m_* = \rho \times V = \frac{4}{3}\pi\rho R_s^3 = \frac{4}{3}\pi(0.8R_{\odot})^2 0.688\rho_{\odot} = 0.44M_{\odot} \tag{3.2.7}$$

Using Kepler's third law, we can find the semi-major axis value of the star's orbit.

3.3 Secondary Star Analysis

As shown by equation 3.2.1, the companion star's can be calculated if the other binary star's radium is obtained.

$$R_{dimmer} = \frac{R_{brighter}}{\sqrt{\delta}} = \frac{0.8R\odot}{\sqrt{0.91}} = 0.83R_{\odot} \tag{3.3.1}$$

From the obtained result by equation 3.3.1, we can see that the secondary star maintains a larger radius than the primary star with a difference of 0.03 solar radii. The closeness between the stars' radius shows that the two objects have a similar volume, explaining observed point dips in 3 as transiting duration is limited to a short time interval.

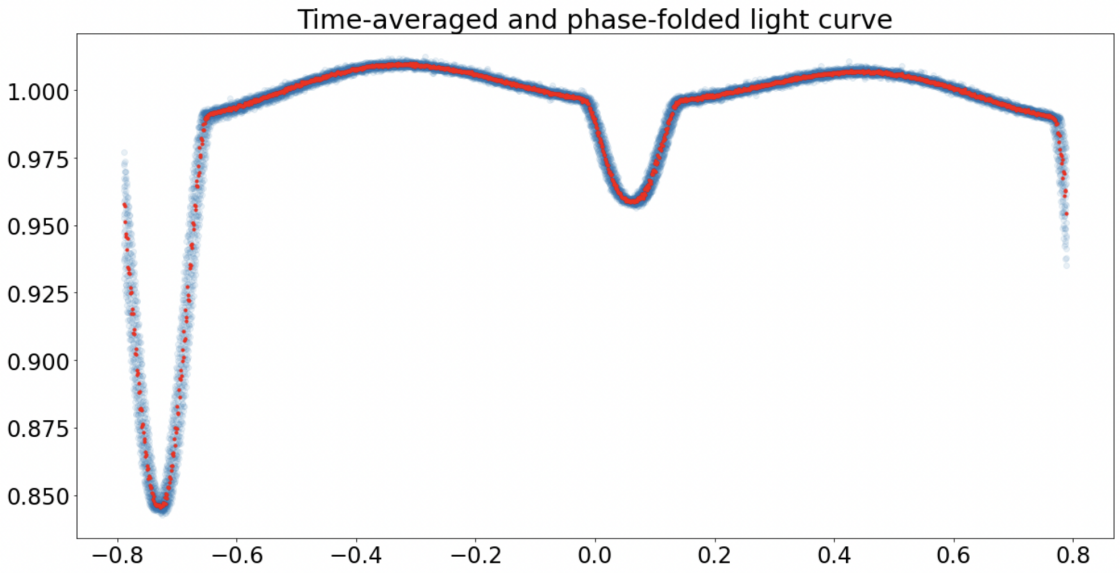

Figure 6: Time-average and phase-folded light curve for TIC 7720507

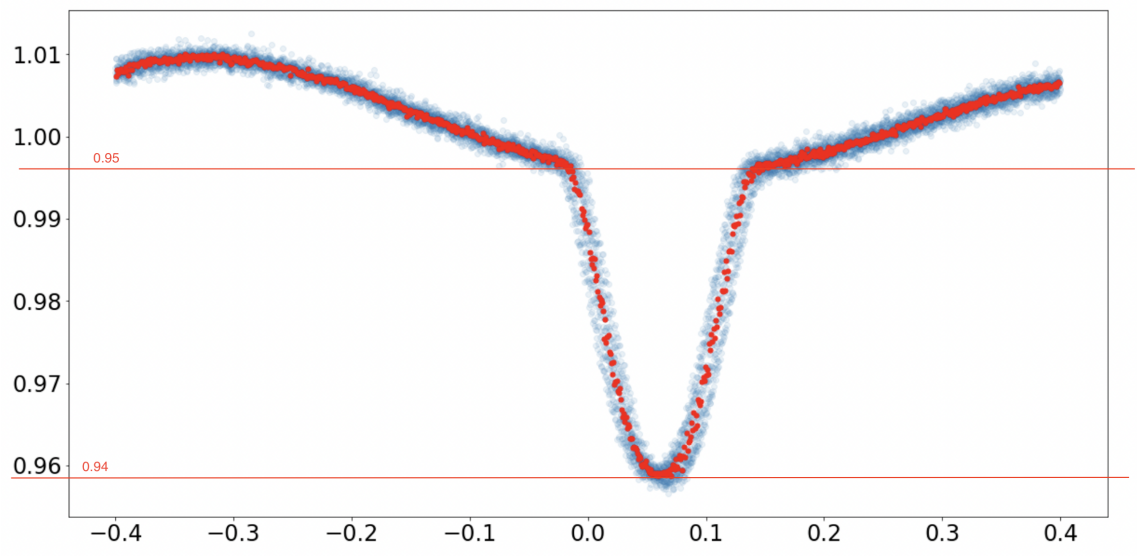

Figure 7: Best fit of the secondary dip's light curve after time-averaged and phase fold

4 Results

4.1 Information about Eclipsing Binaries

By utilizing the transit method and observing timing variations, we conclusively demonstrated that TIC 7220507 is an eclipsing binary system consisting of two stars with a similar size located at 193.337 parsecs. Using the Hertzsprung-Russell diagram, we can conclude the primary star in the system is a F-type main sequence star with a yellow-white color and an effective temperature of 6490 Kelvin, fusing hydrogen that produces radiant power observed by the TESS telescope.

All physical quantities concluded from the investigation is listed in Table 1.

Table 1

Quantities	Astronomical Unit
Period one complete transit	136389.19 sec
Duration of one complete transit	8640 sec
Absolute Magnitude M* of the primary star	$0.51M_{\odot}$
Fractional depth of the secondary eclipse, δ	0.91
Approximated radius of the primary star	$0.80R_{\odot}$
Density of the primary star ρ_*	$0.69\rho_{\odot}$
Mass of the primary star	$0.44M_{\odot}$
Approximated radius of the secondary star	$0.84R\odot$

4.2 Null result for Exoplanet Transits in TESS Eclipsing Binary Systems

In our search we have not encountered any compelling evidence for the presence of exoplanet transits. One major difficulty in detecting exoplanets is their luminosity because planets are much dimmer than the star they orbit and that the orbital periods of exoplanet transits are different from the main eclipsing binary transits, making conventional means of phase-folding counterproductive for exoplanet transit detection in multiple-star systems as exoplanet transits could be visually mistaken for instrumental error or noise resulting from discontinuities in data.

We used the TESS data and programming packages during the investigation to produce a light curve graph for stars to find exoplanets by observing secondary dips. Since transits occur at a different time for each star and some images captured by TESS, contain significant systematic errors due to discontinuity in photographing, identifying dips requires visualizations and cannot be computed by a program at once by selecting a uniform time interval. Therefore, we decide to re-run each star by changing the ID number shown in figure 1 to produce a light curve and select the position where a potential transit occurs. However, since there is a large amount of existing

data on eclipsing binary system candidates and each system can have an exoplanet, there is a slight possibility of detecting exoplanets by creating an independent program for each star.

5 Discussion

Since data from the TESS mission is limited to certain quantities, we use several approximations in the determining physical properties of TIC 7720507, generating random errors that influence the investigation's accuracy. One major error is the estimation of the star radius by eyes using the Hertzsprung-Russell diagram, producing random errors that influence the accuracy as humans reading abilities are limited. Since many quantities are derived from radius with complex calculation process, inaccuracies in the value reduce the accuracy of other results and uncertainties are enlarged. Another approximation we used is when calculating the density of TIC 7720507. To obtain a result with a higher accuracy, we can use the trigonometric function of $\tan\theta$ when calculating θ angle and use this value in later steps. However, considering the large value of a star's radius and its semi-major axis, the difference between $\tan\theta$ and θ should not produce a significant impact on the result accuracy and will be a counted as a secondary error.

The identification of transiting exoplanets among eclipsing binaries has proven to be challenging and prone to mistake due to systematic errors in equipment. We did not identify the further presence of exoplanet transits in eclipsing binary stars via visually analysing its transiting light curves. In order to increase the potential of discovering exoplanet, it is necessary to enhance the efficiency to produce light curves and increase the number of tested data. Due to constraints on time and computational resources, we were unable to establish an efficient system to conduct an exhaustive search on the TESS data; we understand that further research would be required in this area. We acknowledge that more advance machine learning models currently are being develop that aim to automate the process of identifying exoplanet transits among eclipsing binary light curves. (Yu et al.) Automated planet candidate identification has become an attractive alternative to human vetting with the development of better observation instruments that allow unparalleled amounts of data and light curves to be collected.

This paper makes use of data collected by the TESS mission, which are publicly available from the Mikulski Archive for Space Telescopes (MAST). This work makes use of Python and the Python packages lightkurve, Numpy, Scipy, Matplotlib and mandelagol.

References

Javier Barbuzano. Strange exoplanets: The real tatooines. URL skyandtelescope.org.

Anatoliy I Fisenko and Sergey N Ivashov. Determination of the true temperature of molybdenum and luminous flames from generalized wien's displacement and stefan–boltzmann's laws: thermodynamics of thermal radiation. *International Journal of Thermophysics*, 30(5):1524–1535, 2009.

G Giuricin, Fabio Mardirossian, and Marino Mezzetti. Synchronization in eclipsing binary stars. *Astronomy and Astrophysics*, 131:152–158, 1984.

J. D. Hartman and G. Á. Bakos. Vartools: A program for analyzing astronomical time-series data, Oct 2016. URL https://ui.adsabs.harvard.edu/abs/2016A%26C....17....1H/abstract.

Erin L. Howard, James R. A. Davenport, and Kevin R. Covey. 370 new eclipsing binary candidates from TESS sectors 1-26. URL http://arxiv.org/abs/2205.14184.

GP Kuiper. The magnitude of the sun, the stellar temperature scale, and bolometric corrections. *The Astrophysical Journal*, 88:429, 1938.

Francesco Pepe, David Ehrenreich, and Michael R. Meyer. Instrumentation for the detection and characterization of exoplanets. 513(7518):358–366. ISSN 0028-0836, 1476-4687. doi: 10.1038/nature13784. URL https://www.nature.com/articles/nature13784.

Andrej Prsa, Angela Kochoska, Kyle E. Conroy, Nora Eisner, Daniel R. Hey, Luc IJspeert, Ethan Kruse, Scott W. Fleming, Cole Johnston, Martti H. Kristiansen, Daryll LaCourse, Danielle Mortensen, Joshua Pepper, Keivan G. Stassun, Guillermo Torres, Michael Abdul-Masih, Joheen

Chakraborty, Robert Gagliano, Zhao Guo, Kelly Hambleton, Kyeongsoo Hong, Thomas Jacobs, David Jones, Veselin Kostov, Jae Woo Lee, Mark Omohundro, Jerome A. Orosz, Emma J. Page, Brian P. Powell, Saul Rappaport, Phill Reed, Jeremy Schnittman, Hans Martin Schwengeler, Avi Shporer, Ivan A. Terentev, Andrew Vanderburg, William F. Welsh, Douglas A. Caldwell, John P. Doty, Jon M. Jenkins, David W. Latham, George R. Ricker, Sara Seager, Joshua E. Schlieder, Bernie Shiao, Roland Vanderspek, and Joshua N. Winn. TESS eclipsing binary stars. i. short cadence observations of 4584 eclipsing binaries in sectors 1-26. 258(1):16. ISSN 0067-0049, 1538-4365. doi: 10.3847/1538-4365/ac324a. URL http://arxiv.org/abs/2110.13382.

Michael Richmond. What can we learn from transits? URL http://spiff.rit.edu/classes/resceu/lectures/transit_ii/transit_ii.html.

Johanna Teske, Matías R Díaz, Rafael Luque, Teo Močnik, Julia V Seidel, Jon Fernández Otegi, Fabo Feng, James S Jenkins, Enric Pallè, Damien Ségransan, et al. Tess reveals a short-period sub-neptune sibling (hd 86226c) to a known long-period giant planet. *The Astronomical Journal*, 160(2):96, 2020.

K Tran, A Levine, S Rappaport, T Borkovits, Sz Csizmadia, and Belinda Kalomeni. The anticorrelated nature of the primary and secondary eclipse timing variations for the kepler contact binaries. *The Astrophysical Journal*, 774(1):81, 2013.

Liang Yu, Andrew Vanderburg, Chelsea Huang, Christopher J. Shallue, Ian J. M. Crossfield, B. Scott Gaudi, Tansu Daylan, Anne Dattilo, David J. Armstrong, George R. Ricker, Roland K. Vanderspek, David W. Latham, Sara Seager, Jason Dittmann, John P. Doty, Ana Glidden, and Samuel N. Quinn. Identifying exoplanets with deep learning. III. automated triage and vetting of *TESS* candidates. 158(1):25. ISSN 1538-3881. doi: 10.3847/1538-3881/ab21d6. URL https://iopscience.iop.org/article/10.3847/1538-3881/ab21d6.

6 Appendix

The package of "mandelagol" is adopted from Hartman and Bakos (2016)

```
import numpy as np
import matplotlib.pyplot as plt
import lightkurve as lk
from scipy import optimize
from mandelagol import occultquad

result = lk.search_lightcurve("TIC 7720507", mission = "TESS")
result
lc = result[3].download()
lc.scatter()

lc = result[2].download()

lc.filename

lc.scatter()
plt.savefig("flux")
plt.ylim(0,2,5)

lc.scatter()
plt.xlim(1955)
plt.ylim(0,1.4)
plt.savefig("flux")

period = np.linspace(0.5,3.0,1000)
duration = np.linspace(0.01,0.1,10)
bls = lc.to_periodogram(method = 'bls', period = period, duration = duration
    )
bls.plot()
```

```
29
30 period = bls.period_at_max_power
31 t0 = bls.transit_time_at_max_power
32 dur = bls.duration_at_max_power
33 print(period,t0,dur)
34
35 lc.fold(period = period, epoch_time = t0).scatter()
36
37 lc.scatter()
38
39 time = lc.time.to_value('jd')
40 flux = lc.flux.to_value()
41
42 # The following lines get rid of bad data points that contain 'NaN' (not a
       number) values
43 ok = np.isfinite(flux)
44 time = time[ok]
45 flux = flux[ok]
46
47 # Now, let's divide the flux by the median flux, so it is centered around
       1.00
48 flux_norm = flux/np.median(flux)
49
50 plt.figure(figsize=(16,8))
51 plt.plot(time,flux_norm,'.')
52 plt.xlabel('Time [BJD]')
53 plt.ylabel('Relative Flux')
54
55 def time_average(time, flux, npts):
56
57     # input: time, flux, and number of sequential data points that should be
        averaged
58     # output: time_avg and flux_avg.
59     # first make sure the data are sorted in time
60
61     sorted = np.argsort(time)
62     time_sorted = time[sorted]
63     flux_sorted = flux[sorted]
64     ndata = len(time_sorted)
65
66     # now perform the averaging.
67
68     ndata_avg = np.int(ndata/npts) # rounds downward to nearest integer
69
70     time_avg = np.zeros(ndata_avg)
71     flux_avg = np.zeros(ndata_avg)
72
73     for i in range(ndata_avg):
74         i_start = i*npts
75         i_end = i_start + npts
76         time_avg[i] = np.median(time_sorted[i_start:i_end])
77         flux_avg[i] = np.median(flux_sorted[i_start:i_end])
78
79     return(time_avg, flux_avg)
80
81 def calculate_phase(time, period, t0):
82
83     # returns the phase of a periodic function, defined as (time - t0) mod
       period.
84     # the phase ranges from 0 to P, where P is the period.
85     # and the input t0 is used to define where phase=0
86
87     phase = (time - t0) % period  # note, % is the modulo operator
88     last_half = (phase>0.5*period)
89     phase[last_half] = phase[last_half] - period # recenters so that t0
       occurs in the middle
```

```
90
91      return(phase)
92  # period and t0 are obtained from previous steps of the program
93  period = 1.5785785785785786
94  t0 = 2011.3394696247465
95  phase = calculate_phase(time, period, t0)
96
97  plt.plot(phase, flux_norm, 'o', alpha=0.1)
98  phase_avg, flux_avg = time_average(phase, flux_norm, 10)
99  plt.plot(phase_avg, flux_avg, 'r.')
100 plt.title('Time-averaged and phase-folded light curve')
101
102 # Now let's select a portion to fit with a model.
103
104 region_to_fit = (np.abs(phase) <= 0.4)
105 t = time[region_to_fit]
106 f = flux_norm[region_to_fit]
107 ph = phase[region_to_fit]
108
109 plt.plot(ph, f, 'o', alpha=0.1)
110
111 # plot the averaged light curve with red dots to see
112 # how the signal-to-noise ratio has been improved (the fluctuations are
      reduced)
113 ph_avg, f_avg = time_average(ph, f, 10)
114 plt.plot(ph_avg, f_avg, 'r.', markersize=10)
115
116 # Use the standard deviation outside of transits as an estimate of the
      uncertainty in each flux data point
117
118 oot = np.abs(ph) >= 0.2
119 f_oot_std = np.std(f[oot])
120 print("Out of transit standard deviation = ", f_oot_std)
121 f_unc = 0.0*t + f_oot_std
122 plt.errorbar(ph,f,yerr=f_unc,fmt='co',alpha=0.1)
123
124 # Here is the model light curve, using the 'occultquad' function from Mandel
       & Agol
125
126 def transit_lightcurve(params, t, period):
127     t0, k, a, b, u = params
128 #
129 # period = period in days (not a free parameter; it's OK to use an estimate
      from previous work)
130 # t0 = midpoint in BJD_TDB
131 # k = (radius of planet) / (radius of star)
132 # a = (radius of orbit) / (radius of star)
133 # b = transit impact parameter = a*cos(incl)/Rstar
134 # u = limb darkening parameter (0 for uniform intensity, 0.6 for Sun-like)
135 #
136     phi = 2.*np.pi*(t-t0)/period
137     x = a*np.sin(phi)
138     y = b*np.cos(phi)
139     s = np.sqrt(x*x + y*y)
140     flux_calc, flux_no_limb_darkening = occultquad(s,u,0.0,k)
141
142     return(flux_calc)
```